Center for Aeronautical Research

Bureau of Engineering Research
The University of Texas at Austin
Austin, Texas

Report CAR 81-1

MODAL ANALYSIS USING A FOURIER ANALYZER, CURVE-FITTING, AND MODAL TUNING

by

Roy R. Craig, Jr.
Yung-Tseng Chung

NASA Contract No. NAS8-33980
October 1, 1981

MODAL ANALYSIS USING A FOURIER ANALYZER, CURVE-FITTING, AND MODAL TUNING

A Report to

NASA Marshall Space Flight Center

Contract No. NAS8-33980

by

Dr. Roy R. Craig, Jr., Professor

Yung-Tseng Chung, Graduate Research Assistant

Aerospace Engineering and Engineering Mechanics Department

The University of Texas at Austin

Austin, Texas 78712

October 1, 1981

MODAL ANALYSIS USING A FOURIER ANALYZER, CURVE-FITTING, AND MODAL TUNING

Introduction

Since the early 1970's the dominant technique for modal testing of structures has been the use of single-point-excitation, with digital Fourier analysis techniques being employed for determination of frequency response functions (FRF's). Modal parameters (e.g. natural frequencies, damping, mode shapes) are derived from these FRF's by various curve-fitting techniques. Multishaker sine dwell or sine sweep testing, which had predominated prior to the 1970's, became less frequently employed, due to the longer test times and higher equipment costs involved. A few attempts have been made to combine the better features of single-point FFT type testing with multishaker testing. Two notable examples are References (1) and (2).

In Reference (1) Gold and Hallauer employ a Fourier analyzer to acquire single-point-excitation FRF's. Curve-fitting is applied to these in order to determine preliminary modal parameters, from which analytical expressions for the FRF's are obtained. These analytical expressions are then employed as the FRF input to the standard Asher Method of modal tuning.[3,4] The important characteristic of Asher's Method is its capability of tuning individual modes in regions of high modal density. In Reference (1), the evaluation of the modal tuning concept using numerically simulated FRF data was very successful. However, evaluation in an actual modal test produced inconclusive results because of the poor quality of the experimentally-acquired FRF's.

The objective of the modal tuning procedure described in Reference (1) was to provide a procedure for determining accurate modal parameters (natural

frequencies, damping, real normal modes) in situations where high modal density limits the usefulness of single-point-excitation techniques. Reference (2) also employs a tuning procedure for determining modal parameters from FRF's obtained by curve-fitting experimental FRF's. Whereas the original Asher Method[1,3,4] requires output from each shaker (input) location and no other locations, Reference (2) introduces a "minimum coincident response method" which permits the number of response locations to exceed the number of input locations.

In the present work a modal testing, or parameter identification, program which performs the functions indicated in the flow chart of Figure 1 is proposed, and portions of the proposed program are evaluated.

Description of the Program

The proposed modal test program differs from single-input methods widely used at present in that preliminary data may be acquired using multiple inputs, and modal tuning procedures may be employed to define closely-spaced-frequency modes more accurately or to make use of FRF's which are based on several input locations. In some respects the proposed modal test program resembles earlier sine-sweep and sine-dwell testing in that broad-band FRF's are acquired using several input locations, and tuning is employed to refine the modal parameter estimates.

The major tasks performed in the proposed modal test program are outlined in the flow chart in Figure 1. They are: (1) data acquisition and FFT processing, (2) curve-fitting, (3) modal tuning, (4) mathematical modeling, and (5) computer-controlled testing. Phases (1) through (3) are described below, and examples are given to illustrate and evaluate them. Phases (4) and (5) are the subject of further research and program development.

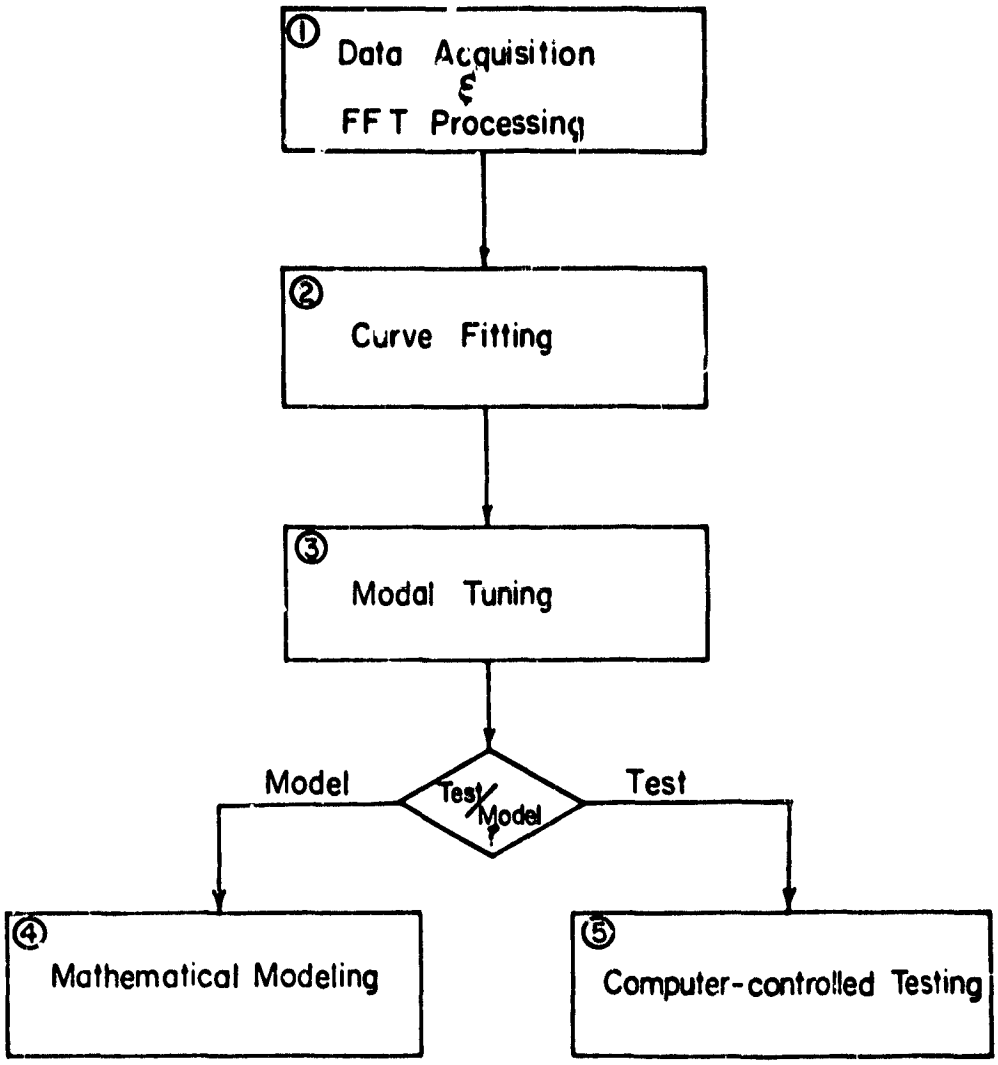

Figure 1. Major Tasks of Proposed Modal Test Program

Data Acquisition and FFT Processing.- This phase of the modal test program, which consists of acquiring FRF's based on several input locations, resembles the broad-band sine sweeps commonly used in the past. However, it is based on FFT processing of excitation and response records. Two forms of data acquisition are available: single-input and multiple-input. Figure 2 snows a dynamical system with m inputs, $x_j(t)$, and n outputs, $y_i(t)$. The single-input data acquisition method involves sequential application of a single shaker at each of the desired m input locations, while the multiple-input method involves operating two or more exciters simultaneously.

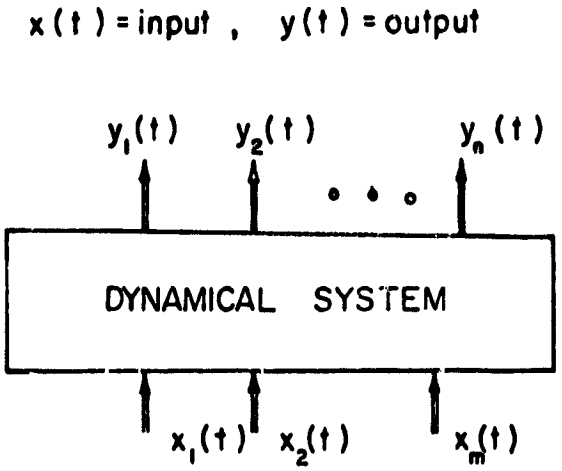

Figure 2. Multiple-Input, Multiple-Output Testing of a Dynamical System

Single-Input Data Acquisition and FFT Processing:

The modal tuning methods to be discussed later require FRF's which are based on two or more input locations. For example, standard Asher tuning using two input locations requires that the FRF's H_{11}, H_{12}, H_{21} and H_{22} be acquired. For minimum coincident response tuning with two inputs and n outputs, the FRF's needed are H_{ij} (i=1,2, ..., n; j=1,2).

For single-input data acquisition, a 2-channel Fourier Analyzer can be used to acquire and process one FRF at a time. Preferably, all response accelerations would be acquired and recorded in a single excitation run, with post-processing to obtain the FRF's.

As with other curve-fitting methods, modal tuning requires a certain frequency resolution in the FRF's if the tuning is to be successful. A data acquisition frequency resolution on the order of one-fourth the half-power bandwidth is desirable. That is,

$$\Delta f \leq \frac{1}{4} (2\zeta f_n) \qquad (1)$$

where ζ is a "representative (viscous) damping factor" (e.g. $\zeta = 0.002$) and f_n is a "representative natural frequency" (e.g. the center frequency of the test frequency band). Frequency resolution will be discussed in more detail later in conjunction with examples of Asher tuning and minimum coincident response tuning.

Multiple-Input Data Acquisition and FFT Processing:

Although single-input FRF's can be used in modal tuning, it is desirable to acquire the FRF's by using multiple-inputs[5,6]. Consider a two-input,

single-output test configuration as shown in Figure 3. (The generalization to multiple-outputs $y_i(t)$ $(i=1,2,\ldots,n)$ is straightforward, but complicates the notation.) Then,

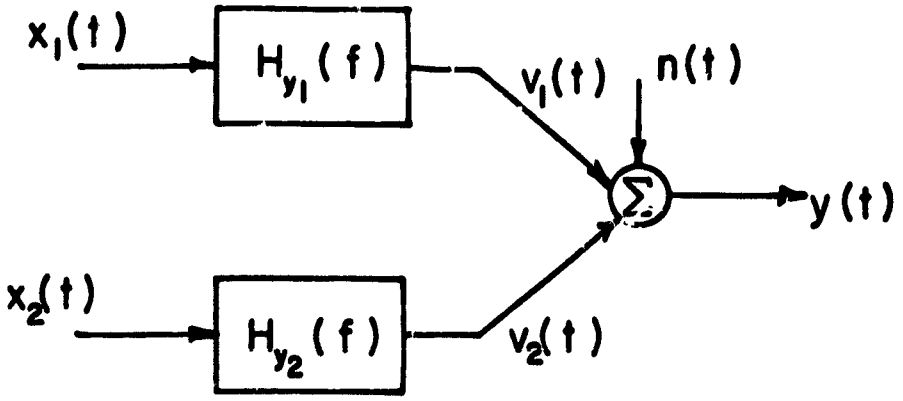

Figure 3. Two-Input, Single-Output System

$$Y(f) = H_{y1}(f)X_1(f) + H_{y2}(f)X_2(f) + N(f) \qquad (2)$$

gives the (Fourier) transformed response, $Y(f)$, due to the two transformed inputs at input coordinates 1 and 2. $N(f)$ is "noise" at the response coordinate which is not linearly related to the inputs. It can be shown[7] that the least-squares estimates for H_{y1} and H_{y2} are obtained by forming

$$YX_1^* = H_{y1}X_1X_1^* + H_{y2}X_2X_1^*$$
$$YX_2^* = H_{y1}X_1X_2^* + H_{y2}X_2X_2^* \quad (3)$$

where it is assumed that averaging is employed and that the noise $N(f)$ is not correlated with either input. Equations (3) can be written

$$G_{y1} = H_{y1}G_{11} + H_{y2}G_{21}$$
$$G_{y2} = H_{y1}G_{12} + H_{y2}G_{22} \quad (4)$$

where the G's are the respective averaged auto- and cross-spectra defined by Equations (3) and (4).

Assume that the ordinary coherence function between inputs $x_1(f)$ and $x_2(f)$ is not equal to unity.

$$\gamma_{12}^2 = \frac{|G_{12}|^2}{G_{11}G_{22}} \neq 1 \quad (5)$$

That is, assume that x_1 and x_2 are not fully correlated. Then Equation (4) may be solved for H_{y1} and H_{y2}.

$$H_{y1} = \frac{G_{y1}G_{22} - G_{y2}G_{21}}{G_{11}G_{22} - |G_{12}|^2} = \left(\frac{G_{y1}}{G_{11}}\right)\left[\frac{1 - \frac{G_{y2}G_{21}}{G_{y1}G_{22}}}{1 - \gamma_{12}^2}\right]$$

$$H_{y2} = \frac{G_{11}G_{y2} - G_{12}G_{y1}}{G_{11}G_{22} - |G_{12}|^2} = \left(\frac{G_{y2}}{G_{22}}\right)\left[\frac{1 - \frac{G_{y1}G_{12}}{G_{y2}G_{11}}}{1 - \lambda_{12}^2}\right] \qquad (6)$$

From equations (5) and (6) it may be seen that when $G_{12} = G_{21}^* = 0$, $\lambda_{12}^2 = 0$, and H_{y1} and H_{y2} are given by the single-input expressions

$$H_{y1} = \frac{G_{y1}}{G_{11}} \quad , \qquad H_{y2} = \frac{G_{y2}}{G_{22}} \qquad (7)$$

In theory, Equations (6) may be employed to obtain FRF's when two inputs are acting simultaneously, so long as the inputs are not fully correlated. The above analysis can be extended to an arbitrary number of inputs and arbitrary number of outputs[5,8]. However, if the ordinary coherence is unity, Equations (6) do not hold, and a different analysis is required.

The advantages of multi-shaker testing have been discussed in References (5) and (6). In the present situation, where modal tuning is to be employed, there is an added advantage to using simultaneous multi-input testing to obtain the FRF's, since the shakers can later be employed for an actual tuned-dwell test based on the results of the modal tuning.

Curve-Fitting for Preliminary Modal Parameter Estimates. - As noted by Gold and Hallauer[1], useful results can be obtained by applying Asher tuning to analytically-synthesized FRF's rather than to the original experimentally-obtained FRF's. Preliminary studies[9] have indicated that it is important to include residual terms in the curve-fitting to obtain parameters for use in analytically synthesizing FRF's which are to be used in modal tuning.

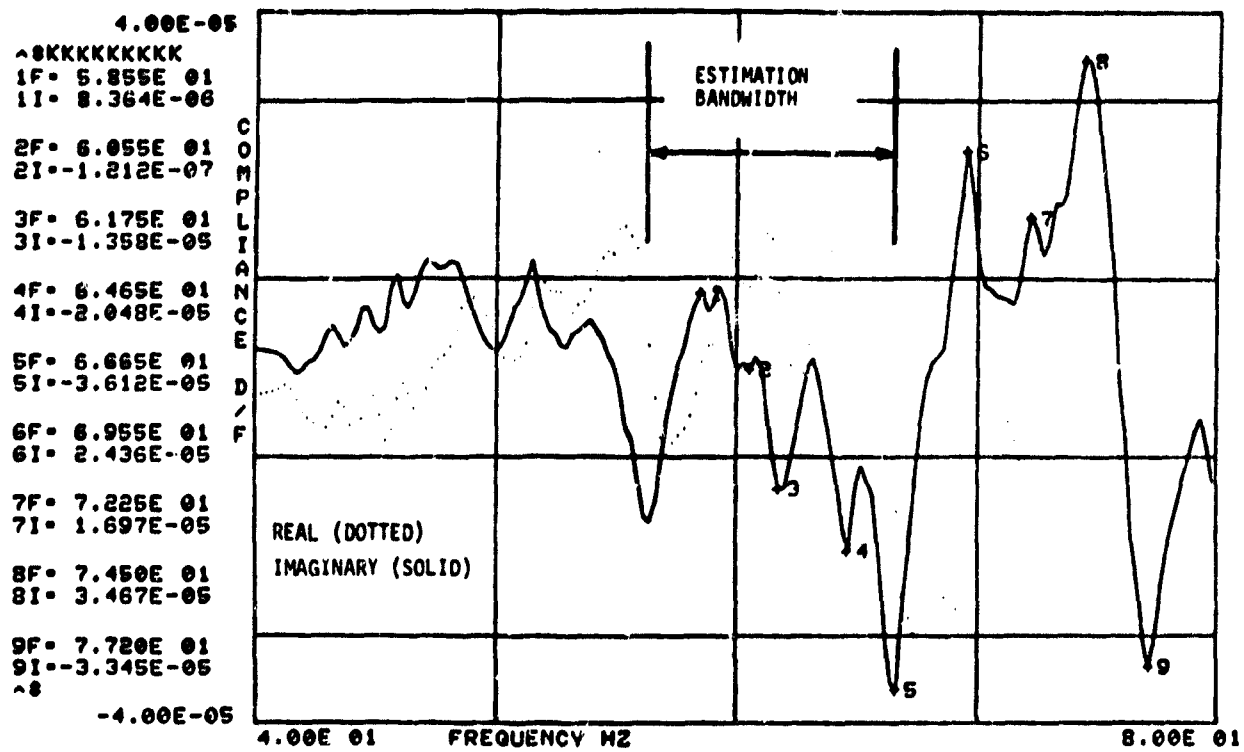

Figure 4. Typical Frequency Response Measurement

Figure 4 shows a typical measured FRF and the frequency band of interest, i.e. the frequency band over which it is desired to "match" the measured FRF by a synthesized FRF. For general viscous damping a

frequency response function for input $x_j(t)$ and output $y_i(t)$ can be written[10]

$$H_{ij}(f) = \frac{Y_i(f)}{X_j(f)} = \sum_{r=1}^{n} \left[\frac{A_{ijr}}{j2\pi f - s_r} + \frac{A_{ijr}^*}{j2\pi f - s_r^*} \right] \quad (8)$$

where

$s_r = -\sigma_r + j\omega_{dr}$

ω_{dr} = damped natural frequency of the r^{th} mode

σ_r = decay rate of r^{th} mode

A_{ijr} = complex residue of the r^{th} mode

$= U_{ijr} + jV_{ijr}$

n = order of the curve fit

Equation (8) can also be written

$$H_{ij}(f) = \sum_{r=1}^{n} \frac{1}{2} \left[\frac{C_{ijr} e^{j\phi_{ijr}}}{(\omega_{dr} - 2\pi f) + j\sigma_r} + \frac{C_{ijr} e^{-j\phi_{ijr}}}{(\omega_{dr} + 2\pi f) - j\sigma_r} \right] \quad (9)$$

where C_{ijr}, ϕ_{ijr}, ω_{dr} and σ_r are all real numbers.

Although for a real system the number of modes, n, is infinite, only a limited number of modes can be employed in the analytically-synthesized FRF. On the other hand, as shown in Figure 4, the frequency band of interest may be from f_a to f_b, and in this range the number of modes is finite. An expression like Equation (8) or Equation (9) can be used to fit the measured FRF in the frequency band of interest, and residuals can be employed to approximate the contributions of modes whose frequencies lie below f_a or above f_b. Then, Equation (8) can be written

$$H_{ij} = L_{ij} + \sum_{r=r_a}^{r_b} \left(\frac{A_{ijr}}{j\omega - s_r} + \frac{A_{ijr}^*}{j\omega - s_r^*} \right) + Z_{ij} \qquad (10)$$

where

ω = $2\pi f$

r_a = lower mode index of frequency range of interest

r_b = upper mode index of frequency range of interest

L_{ij} = lower residual term

Z_{ij} = upper residual term (residual flexibility)

The lower residual term can also be written[10]

$$L_{ij} = -\frac{Y_{ij}}{\omega^2} \qquad (11)$$

where

Y_{ij} = inertia restraint

Thus, with the lower and upper residual terms approximated by use of the real constants Y_{ij} (inertia restraint) and Z_{ij} (residual flexibility), the frequency response function H_{ij} is approximated by

$$H_{ij} = -\frac{Y_{ij}}{\omega^2} + \sum_{r=r_a}^{r_b} \left(\frac{A_{ijr}}{j\omega - s_r} + \frac{A_{ijr}^*}{j\omega - s_r^*} \right) + Z_{ij} \qquad (12)$$

Reference(10) gives additional forms for H_{ij} which are equivalent to Equation (12). For each mode included in the summation there are four real constants. Hence, if N modes correspond to the frequency range from r_a to r_b, then H_{ij} is defined analytically by $4N+2$ real constants. These constants may be obtained by application of a curve-fit algorithm such as the MDOF curve-fit algorithm in the MODAL-PLUS program.

In the section on Examples it will be shown that obtaining analytical FRF's by curve-fitting experimental FRF's prior to modal tuning serves three important functions--it provides initial estimates of natural frequencies, it permits interpolation between experimental data points to establish more accurate natural frequencies, and it permits residuals to be employed so that "resonant modes" can be tuned. If desired, curve-fitting can also be used to generate columns of the FRF matrix corresponding to response locations where no physical input was applied. This was done in Reference (2), where a full FRF matrix was generated from single-point experimental FRF's.

Modal Tuning for Refined Modal Parameter Estimates. - As indicated in the Introduction, modal tuning is to be employed to refine the modal parameter estimates, especially where there are closely-spaced natural frequencies.

Figure 5 shows $I(H_{11})$ and $I(H_{21})$ for a simple analytical 2DOF system with $f_1 = 5.00$ Hz, $f_2 = 5.01$ Hz, $\zeta_1 = 0.01$, and $\zeta_2 = 0.01$. The $I(H_{11})$ curve would seem to indicate a single mode at 5.00 Hz, while the $I(H_{21})$ curve indicates modes at 4.98 Hz and at 5.04 Hz. Allemang[5,6] and other authors have proposed various means for reconciling such apparent "inconsistencies" in modal parameters based on FRF's from two or more response coordinates. The approach employed here is to use modal tuning to isolate the closely-spaced-frequency modes, which are frequently the source of such apparent inconsistencies.

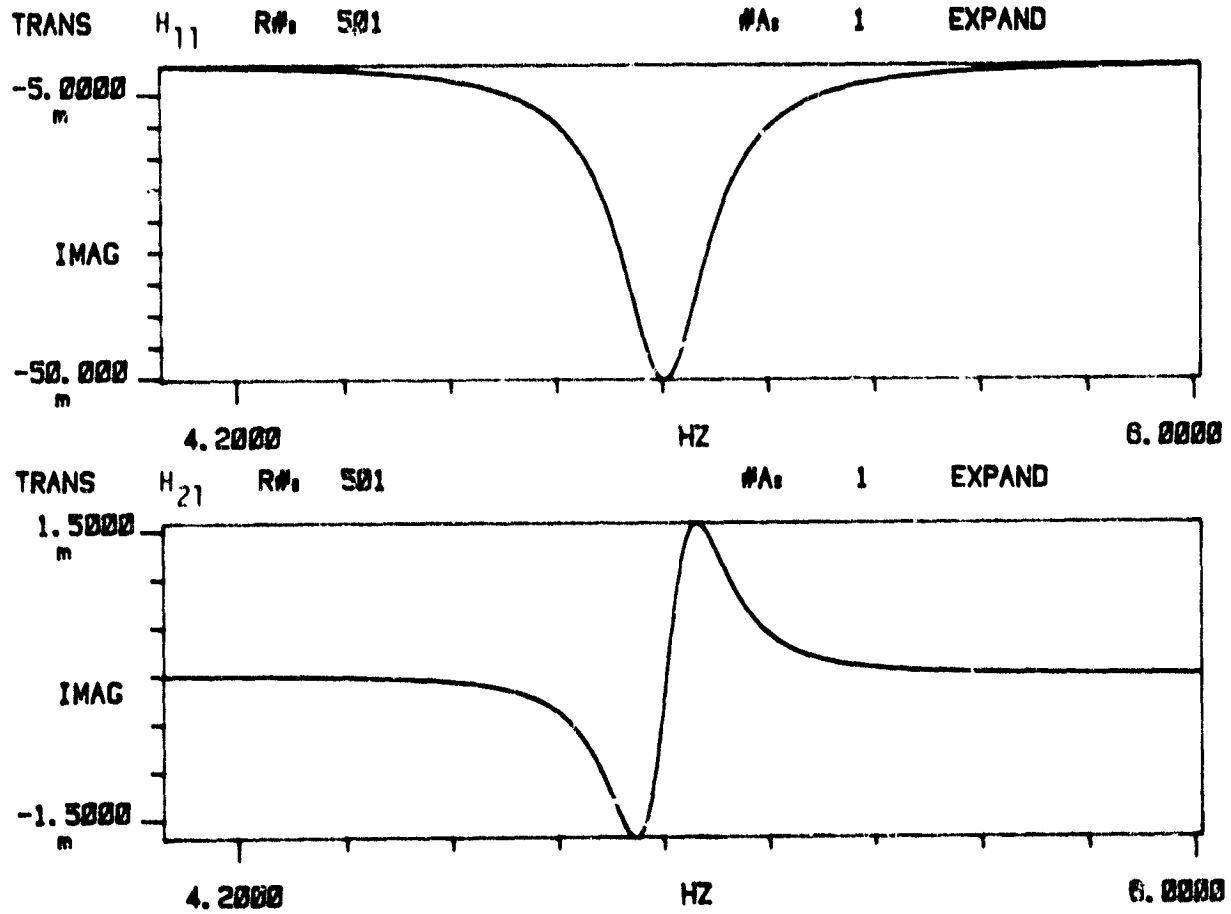

Figure 5. Imaginary Parts of H_{11} and H_{21} for System with Modes at 5.00 Hz and 5.01 Hz.

Standard Asher Method of Modal Tuning:

As indicated in the Introduction, both the standard Asher Method introduced in Reference 3 and a "minimum coincident response method" discussed in Reference 2 will be employed in the present study. (Note: Reference 1 applies the term "standard Asher Method" only to the use of directly-measured FRF's for Asher tuning. Here we will apply the term more generally to tuning using the method described in Reference 3, whether on directly-measured FRF's or on analytically-synthesized FRF's.)

Application of the standard Asher Method of modal tuning begins with either measurement of a pxp FRF matrix, $[\hat{H}]$, over the frequency band of interest, or the synthesis of the $[\hat{H}]$ matrix from modal parameters obtained by curve-fitting the measured data. The linear relationship between the p output transforms and the p input transforms is

$$\underset{pxl}{\{\hat{Y}\}} = \underset{pxp}{[\hat{H}]}\ \underset{pxl}{\{\hat{X}\}} \tag{13}$$

The caret indicates vectors and matrices restricted to the p input/output locations. Next, $[\hat{H}]$ is separated into its real (coincident) and imaginary (quadrature) parts, represented by $[\hat{C}]$ and $[\hat{Q}]$ respectively, giving

$$[\hat{H}] = [\hat{C}] + j\ [\hat{Q}] \tag{14}$$

Equations (13) and (14) may be combined to give

$$\{\hat{Y}\} = [\hat{C}]\{\hat{X}\} + j[\hat{Q}]\{X\} \tag{15}$$

If the input is assumed to be monophase, i.e. all components of $\{\hat{X}\}$ are either in-phase or 180^{o} out-of-phase, then $\{\hat{X}\}$ can be assumed to

be a real vector at each frequency. Then, the response has real and imaginary parts

$$R\{\hat{Y}\} = [\hat{C}]\{\hat{X}\}$$
$$I\{\hat{Y}\} = [\hat{Q}]\{\hat{X}\} \tag{16}$$

It has been shown[2,4] that if $p = n$ = the total number of degrees of freedom of a system, and if f_c and $\{X(f_c)\}$ are chosen to satisfy

$$\underset{nxn}{[C(f_c)]}\ \underset{nx1}{\{X(f_c)\}} = \underset{nx1}{\{0\}} \tag{17}$$

then each f_c satisfying Equation (17) corresponds to an undamped natural frequency of the system, and each corresponding $\{Y(f_c)\}$ is an undamped free vibration mode shape. However, when $p<n$, Equation (17) becomes

$$\underset{pxp}{[\hat{C}(\hat{f}_c)]}\ \underset{px1}{\{\hat{X}(\hat{f}_c)\}} = \underset{px1}{\{0\}} \qquad p < n \tag{18}$$

For a nontrivial solution of this eigenproblem, it is necessary for the determinant of $[\hat{C}]$ to vanish, i.e.

$$\det\ [\hat{C}(\hat{f}_c)] = 0 \tag{19}$$

Some of the roots, $\hat{f}_c$, will be excellent approximations to the true undamped natural frequencies of the system, but some will be "spurious frequencies." "Spurious frequencies" can be distinguished from true

frequencies either by employing several different sets of input/response stations[4], or by examining the phase of the response at points other than the p input points. It has also been observed[1] that when $\det [\hat{C}(f)]$ is plotted versus f, steep crossings of the frequency axis are generally excellent approximations of true system frequencies. Newton's iteration method may be employed in solving for the roots in Equation (19).

$$f_{h+1} = f_h - D_h \frac{f_h - f_{h-1}}{D_h - D_{h-1}} \tag{20}$$

where $D_h = \det[\hat{C}(f_h)]$.

Having identified the approximate natural frequency $\hat{f}_c$ of a mode and having calculated $[\hat{C}(\hat{f}_c)]$ from the FRF synthesizing equation, e.g. Equation (12), we next determine the amplitude of the shaker forces necessary to tune this mode. This distribution is calculated from Equation (18). A narrow-band sweep about $\hat{f}_c$ with fixed $\hat{X}(f) = \hat{X}(\hat{f}_c)$ can be performed analytically, and refined modal parameters can then be determined.

Minimum Coincident Response Method of Modal Tuning:

Invariably the number of response points exceeds the number of excitation points, even in a multi-shaker sine-sweep or sine-dwell test, and the modal amplitudes at many of these points may be of the same order of magnitude as the modal amplitudes at the excitation points. The minimum coincident response method introduced in Reference (2) permits information from non-input points to be accounted for in the process of tuning for undamped free vibration modes.

Let Equation (13) be expanded to include q response points, while the number of input points is $p < q$, and let the resulting equation be written

$$\underset{qx1}{\{\tilde{Y}\}} = \underset{qxp\ px1}{[\tilde{H}]\{\tilde{X}\}} = \underset{qxp\ px1}{[\tilde{C}]\{\tilde{X}\}} + \underset{qxp\ px1}{j[\tilde{Q}]\{\tilde{X}\}} \tag{21}$$

As before, we assume that $\{\tilde{X}\}$ is real. Then

$$R\{\tilde{Y}\} = \{\tilde{Y}\}_R = [\tilde{C}]\{\tilde{X}\} \tag{22}$$

However, since $[\tilde{C}]$ is not a square matrix, it is not possible to determine unique frequencies and force appropriations in the same manner as was done in Equations (18) and (19). In Reference (11) Ibañez discussed this problem and suggested the use of a pseudo-inverse. Here, however, we will employ the least-squares error procedure introduced by Ensminger and Turner in Reference (2).

Let the error function be the sum of the squares of the coincident (real) responses, i.e.

$$\epsilon = \{\tilde{Y}\}_R^T \{\tilde{Y}\}_R = \{\tilde{X}\}^T[\tilde{C}]^T [\tilde{C}] \{\tilde{X}\} \tag{23}$$

be minimized subject to the condition

$$\tilde{Y}_{iR} = [\tilde{C}]_i \tilde{X} = 1 \tag{24}$$

where

$$[\tilde{C}]_i = i^{th} \text{ row of } [\tilde{C}] .$$

The procedure employed by Reference (2) is to minimize the error with respect to the components of the input $\{X\}$ at each frequency f ; then to determine the corresponding values of $\varepsilon(f)$ and to select those frequencies $\tilde{f}_c$ which correspond to minima of $\varepsilon(f)$ as the natural frequency estimates. The expression for $\{\tilde{X}(f)\}$ which minimizes $\varepsilon(\{\tilde{X}\}, f)$ for a specified f is[2]

$$\{\tilde{X}\} = \frac{1}{\lfloor\tilde{C}\rfloor_1(\tilde{C}^T\tilde{C})^{-1}\lfloor\tilde{C}\rfloor_1^T}\,(\tilde{C}^T\tilde{C})^{-1}\,\lfloor\tilde{C}\rfloor_1^T \qquad (25)$$

Equation (25) is used to compute $\{\tilde{X}(f)\}$, and then Equation (23) is employed to compute the resulting least-squares error.

Program Verification

In Figure 1 the major tasks performed in the proposed modal test program were outlined: (1) data acquisition and FFT processing, (2) curve-fitting, (3) modal tuning, (4) mathematical modeling, and (5) computer-controlled testing. An analytical model has been formulated and an experimental model has been fabricated for use in checking out the first three of these tasks.

Experimental Model. - Since most experimental modal testing is done on structures whose modal properties are unknown at the outset and for which there is no validated mathematical model, it was decided to construct a relatively simple physical model to be used in evaluating the various phases of the proposed modal testing program prior to application of the techniques

to "real hardware." Figure 6 shows the basic elements of the lightly-coupled 2-beam structure constructed. The structure consists of two aluminum box beams 1.52m long, to which damping material (one constrained layer and one non-constrained layer) has been applied, and which are coupled by two torsion rods, which may be various lengths and various materials. To increase the modal density, tuned "outrigger beams" are attached to the main beams. Both coupling torsion bars and outrigger beams are attached to the main beams near the node points of the fundamental free-free bending mode of the main beams. Figure 7 shows a single main beam with outriggers and with two shakers attached to the beam by long "push rods." Figure 8 shows a closeup of the force cell and accelerometer attachments at the end of the box beam. Also shown is an outrigger beam, which is cantilevered from the bottom of the main beam. After several unsuccessful attempts to obtain FRF's with two shakers operating simultaneously, the setup was modified by inserting a block at each end of the main beams to prevent local deformation of the end cross-sections. The long push rods were replaced by shorter shaker attachment fittings. Figure 9 shows a test configuration with two main beams, but with the outrigger beams removed and the shaker attachments made more directly.

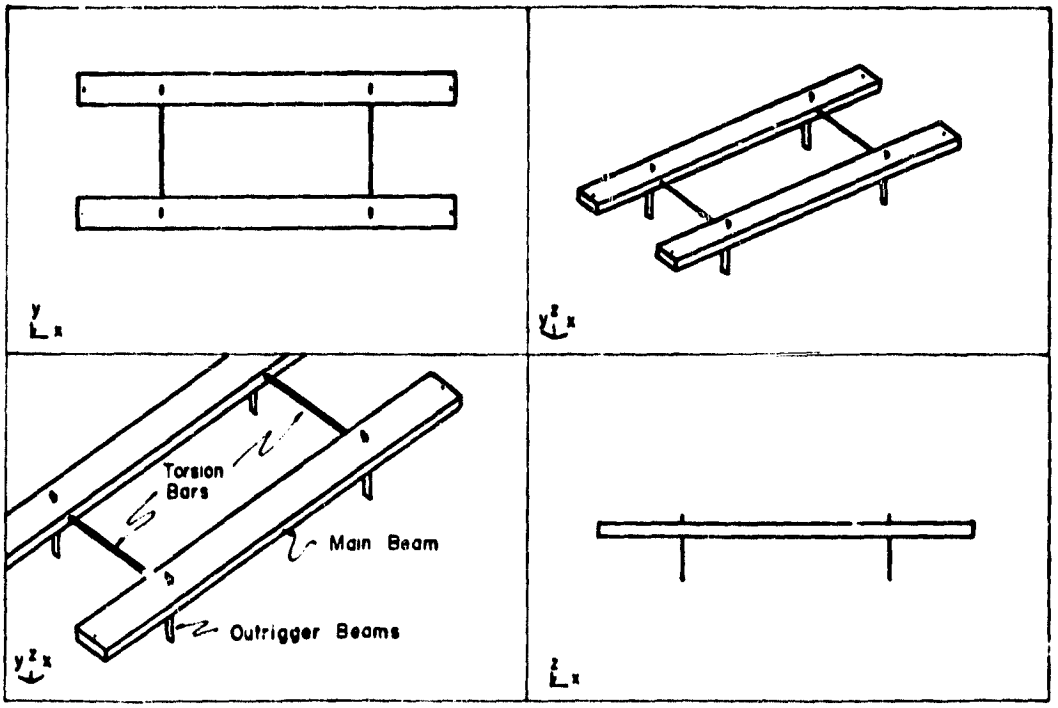

Figure 6. 2-Beam Test Structure with Outrigger Beams

Figure 7. Single Beam with Major Instrumentation

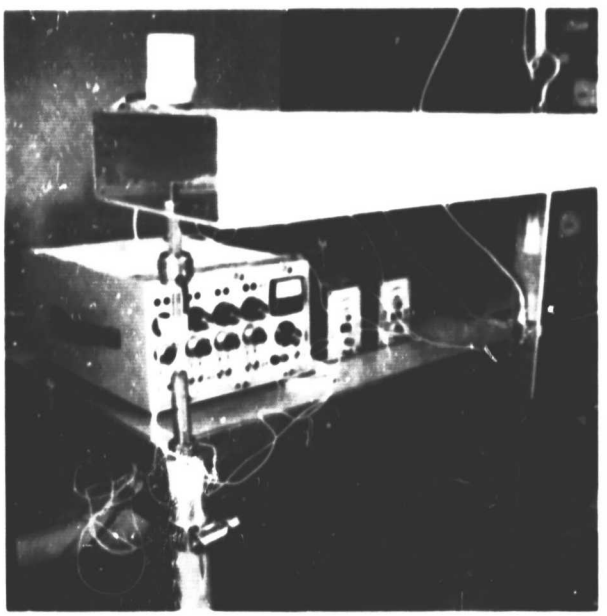

Figure 8. Original Force Cell and Accelerometer Attachments

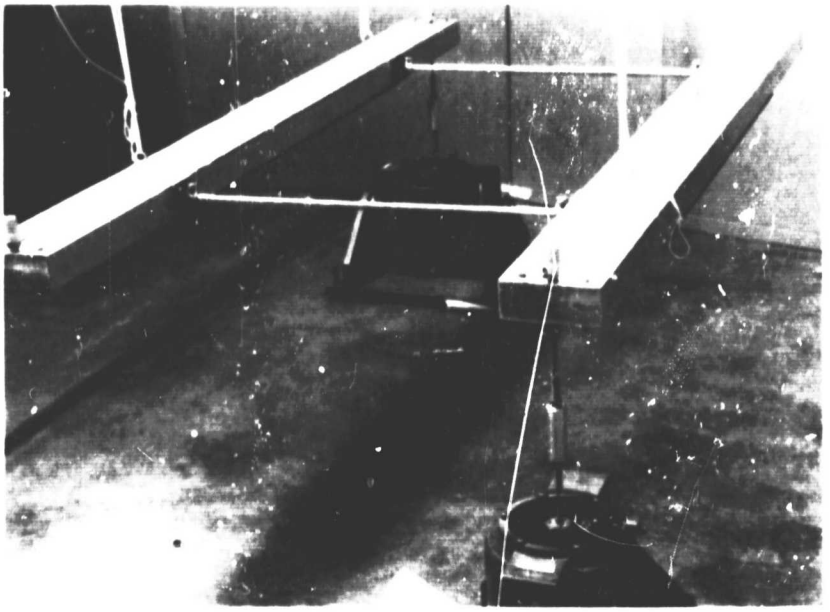

Figure 9. Dual-Beam with Modified Ends and Modified Shaker Attachment

Instrumentation. - The instrumentation listed in Table 1 has been employed for excitation of the structure, recording analog signals, performing data acquisition and FFT processing, and performing the computations associated with curve-fitting, modal tuning, etc.

Item	Model
Accelerometers	Endevco, 2265-20
Accelerometers	PCB, 308B
Force cells	PCB, 208-A02
Signal conditioners	Vishay, 2120
Analog tape recorder	Hewlett-Packard (Sanborn), 3900
Electrodynamic shakers (50 lb.)	MB, MB1500
Fourier analyzer	Hewlett-Packard, 5420A
Desktop computer	Hewlett-Packard, 9825A
Pen plotter	Hewlett-Packard, 7225
Digital computer	Digital Equipment, PDP11/60

Table 1. Equipment List

For single-shaker testing, the Hewlett-Packard 5420A was used both to provide a random voltage signal to the shaker amplifier and to acquire analog force and acceleration signals and produce FRF's. For 2-shaker testing, the tape recorder was used to supply two pre-recorded uncorrelated random voltage signals to the shaker amplifiers and to record the resulting analog force and acceleration signals. A trigger signal was also recorded

on the tape so that proper phase relationships could be maintained when the 5420A was subsequently used to produce auto-spectra and cross-spectra for use in computing FRF's using Equations (6). The 9825A desktop computer was used for these FRF calculations and for the modal tuning calculations, while the PDP11/60 was used for curve-fitting the experimental FRF's.

Examples. - Examples will be presented to illustrate the following: calculation of FRF's based on dual-shaker excitation, curve-fitting of experimental FRF's, standard Asher tuning, and minimum phase error tuning.

Multi-shaker Excitation:

Tests were conducted using dual-shaker excitation of the following experimental models: (1) single-beam configuration as shown in Figure 7, (2) dual-beam configuration with outriggers, with teflon torsion bars connecting the two main beams, and with long shaker push rods, and (3) dual-beam configuration shown in Figure 9. As noted before, the analog tape recorder was used to record the two force channels and the two accelerometer channels. These records were played back as input to the HP 5420A, which was used to compute the auto-spectra and cross-spectra required to compute γ^2_{12}, H_{11}, H_{12}, H_{21} and H_{22} using Equations (5) and (6). Data are presented below for the two dual-beam configurations, (2) and (3), described above.

A dual-shaker test of configuration (2) produced the data shown in Figures 10(a) through 10(g). Figures 10(a) and 10(b) are the two force auto-spectra, Figure 10(c) shows the ordinary coherence between the two force channels, and Figures 10(d) through 10(g) show the real and imaginary parts of H_{11} and H_{61}, where coordinates 1 and 6 are the opposite-corner

shaker locations (e.g. see Figure 9). Although H_{11} is quite similar to the H_{11} produced by a single-shaker test, it is apparent that H_{61} is too "noisy" to be an acceptable FRF. Since the force coherence is not equal to unity, Equations (6) are valid over the entire frequency range. The two force autospectra plots, Figures 10(a) and 10(b), indicate that in the vicinity of structural resonances, the excitation levels were very low. However, these autospectra are quite similar to those obtained in single-shaker tests of the same structure.

Several further attempts to compute FRF's based on data taken for configuration (2) did not produce any more acceptable FRF's than those in Figures 10(d) through 10(g). Several changes were then made to the experimental model, resulting in the structure shown in Figure 9. End blocks were installed in the main beams to provide stiffer attachment locations for the force cells and accelerometers, and the aluminum shaker "push rods" were removed, permitting the more direct shaker attachment shown in Figure 9. Some results obtained for this test configuration are shown in Figures 11(a) through 11(g). Figures 11(a) through 11(c) show the two force auto-spectra and the ordinary force coherence, while Figures 11(d) through 11(g) give H_{11} and H_{61}. For comparison, Figure 12(a) is the force auto-spectrum for a single-shaker test of this structure with the shaker at coordinate 1, while Figures 12(b) through 12(e) are the real and imaginary plots for the single-shaker FRF's H_{11} and H_{61}. A cursory comparison of Figures 11 and 12 would seem to indicate that the single-shaker FRF's are more accurate. Since significant improvement in the dual-shaker FRF's was achieved by making

changes in the shaker attachment fixturing, it seems likely that further improvements in the dual-shaker FRF's could be achieved by improvements of technique.

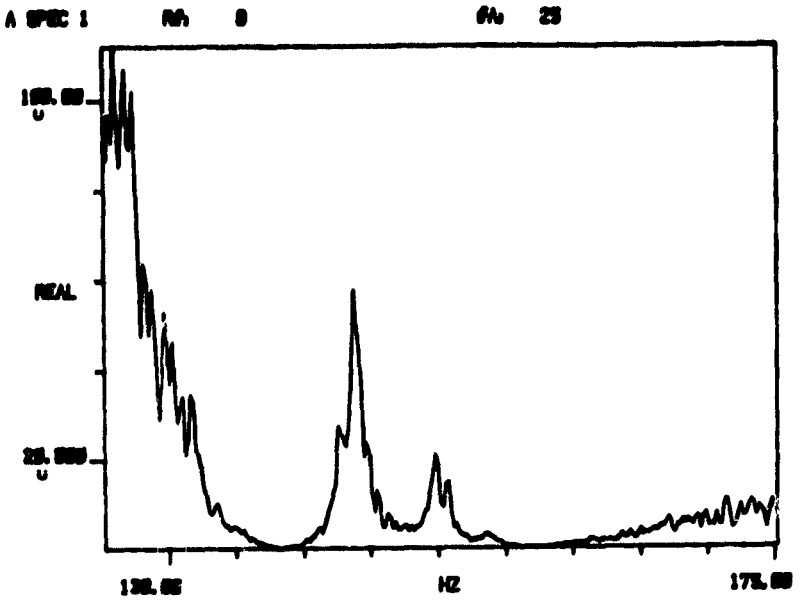

Figure 10a. Force Autospectrum for Shaker No. 1

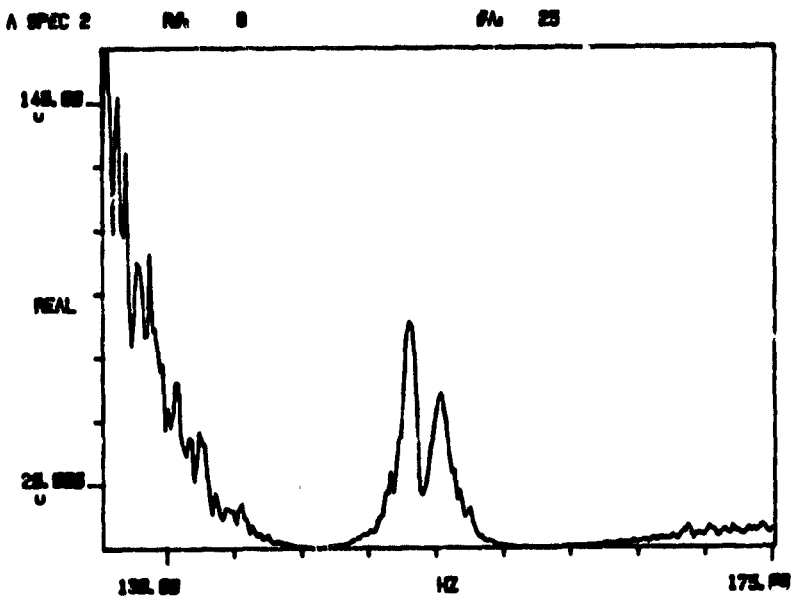

Figure 10b. Force Autospectrum for Shaker No. 2

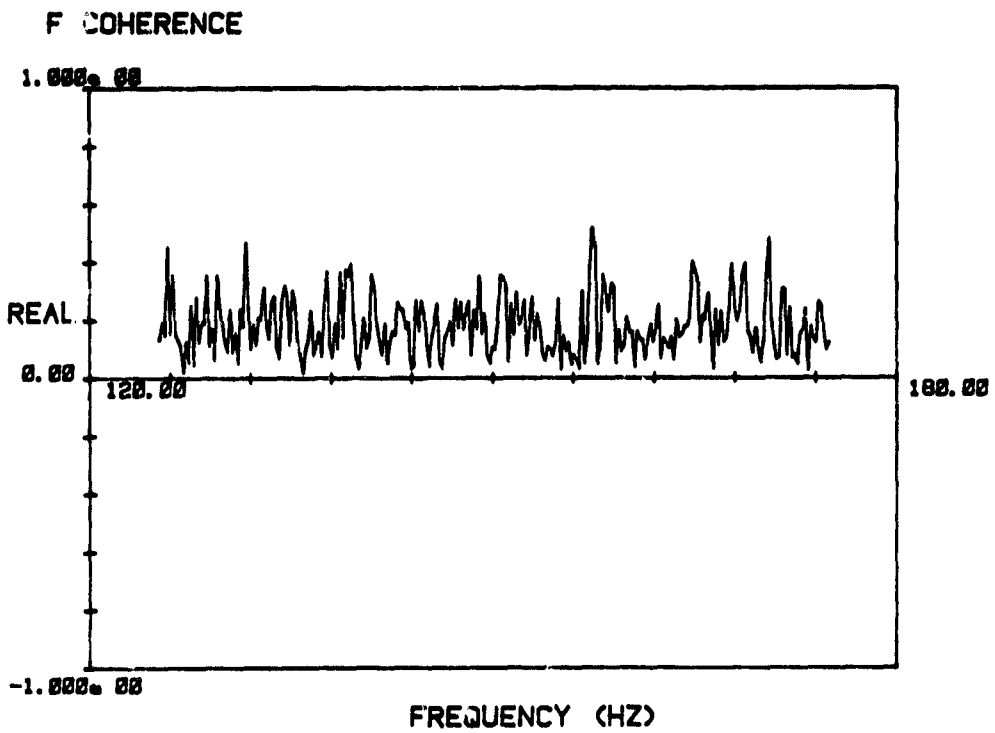

Figure 10c. Ordinary Coherence Between Shaker No. 1 Force and Shaker No. 2 Force

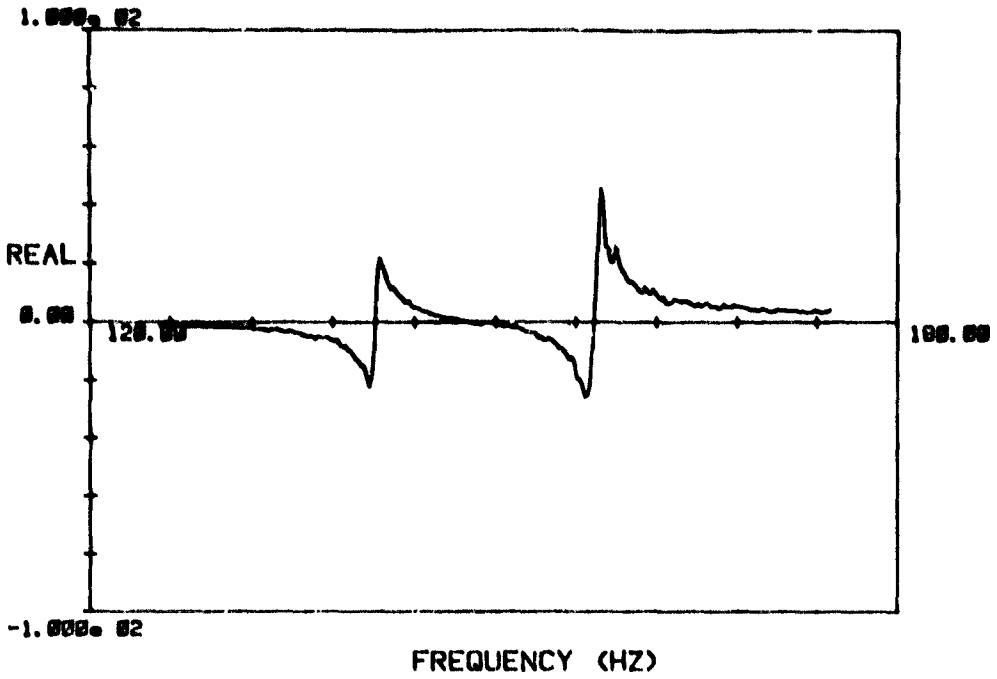

Figure 10d. Real Part of H_{11}. Configuration (2).

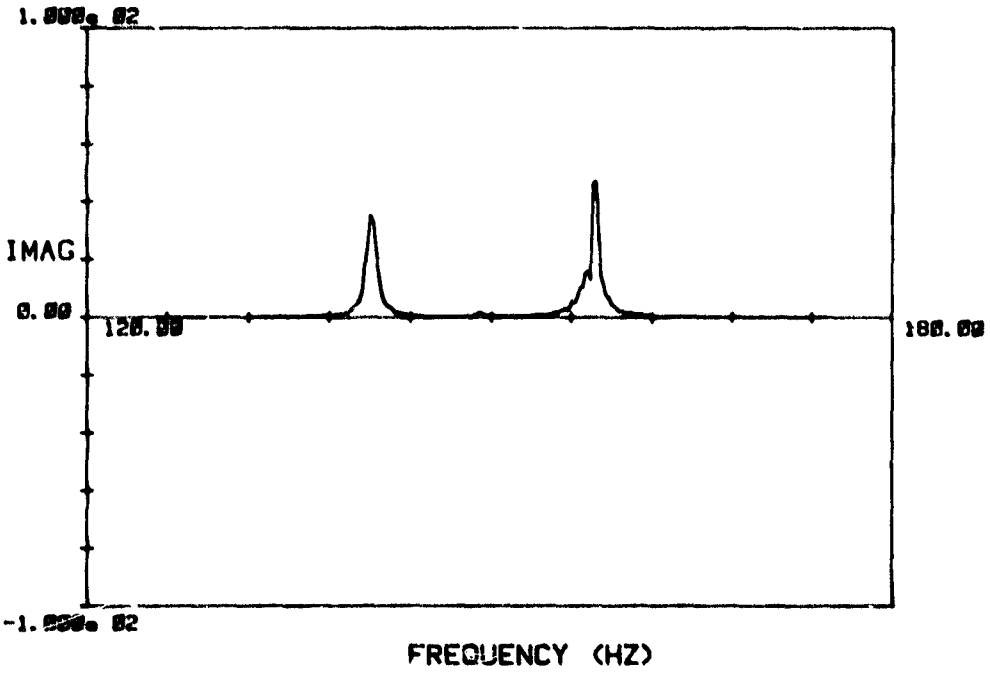

Figure 10e. Imaginary Part of H_{11}. Configuration (2).

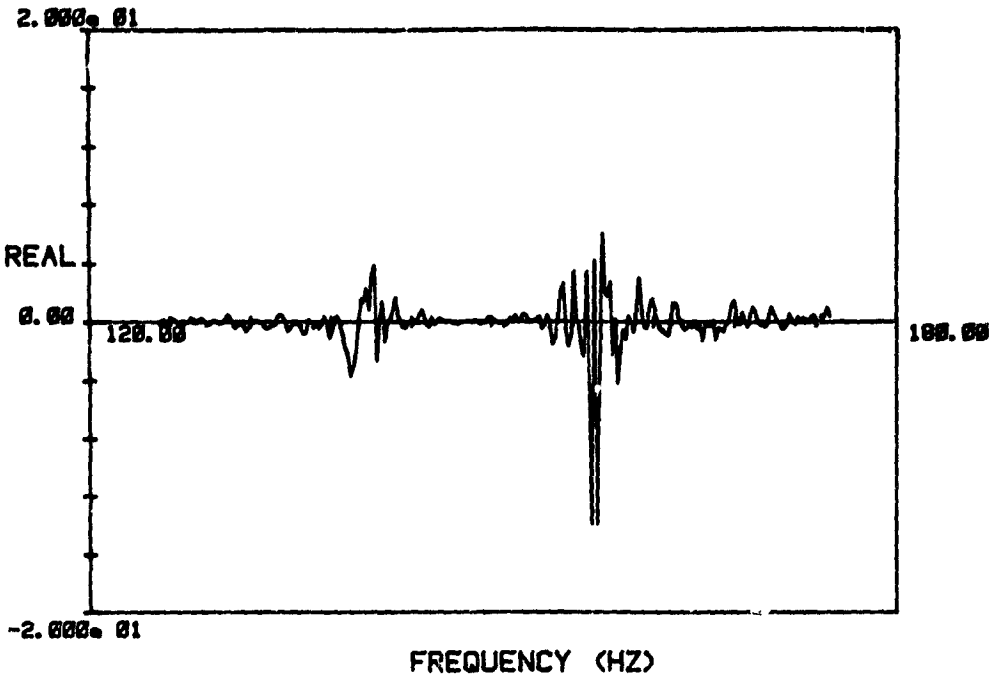

Figure 10f. Real Part of H_{61}. Configuration (2).

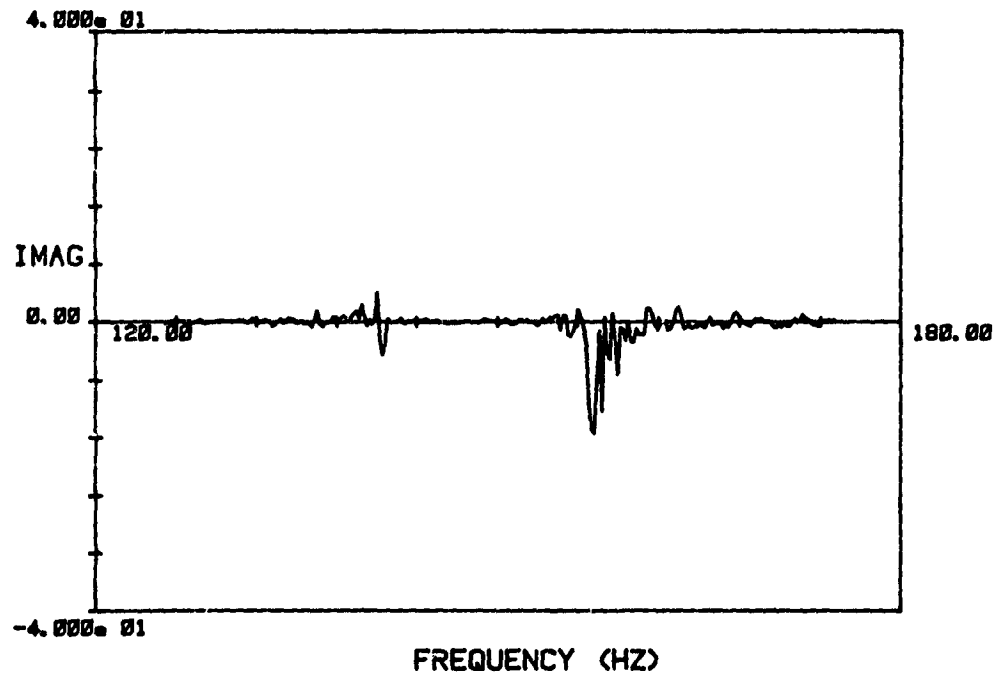

Figure 10g. Imaginary Part of H_{61}. Configuration (2).

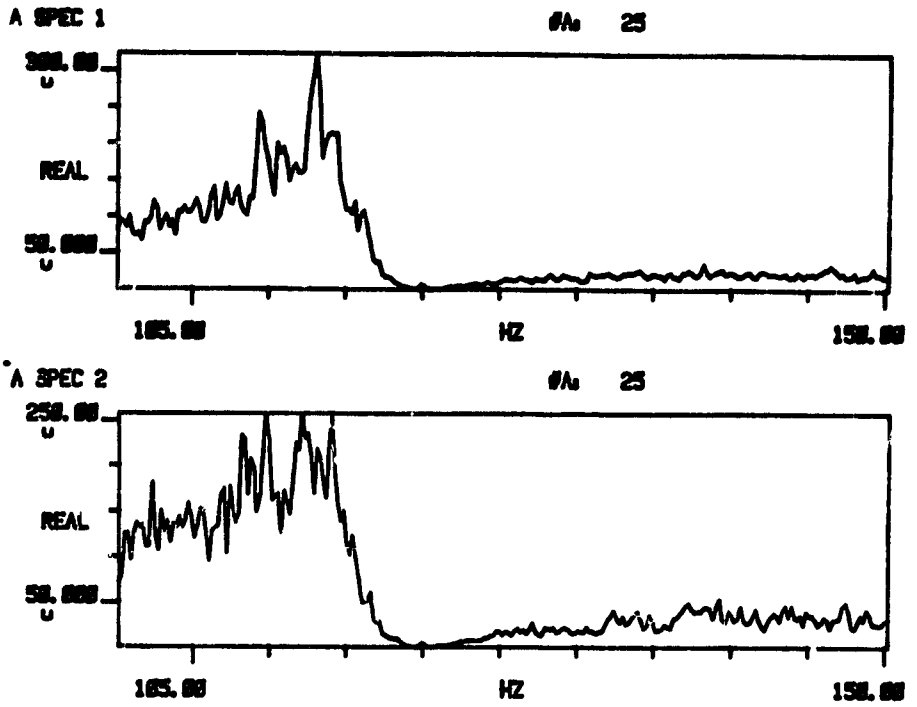

Figures 11a,b. Force Autospectra. Configuration (3).

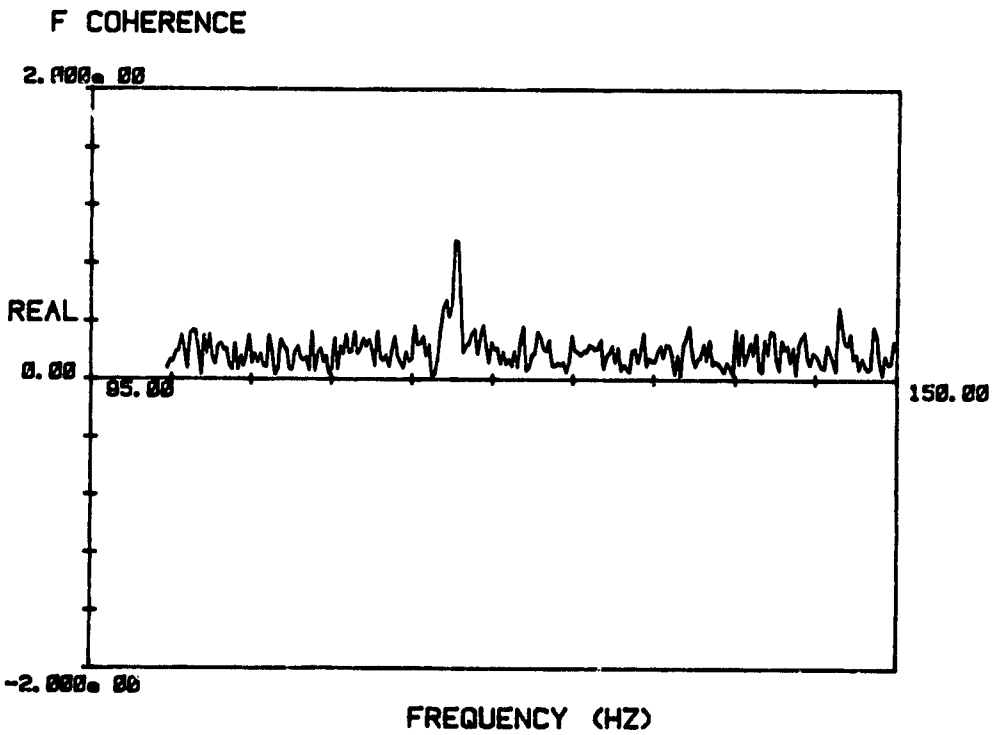

Figure 11c. Ordinary Force Coherence. Configuration (3).

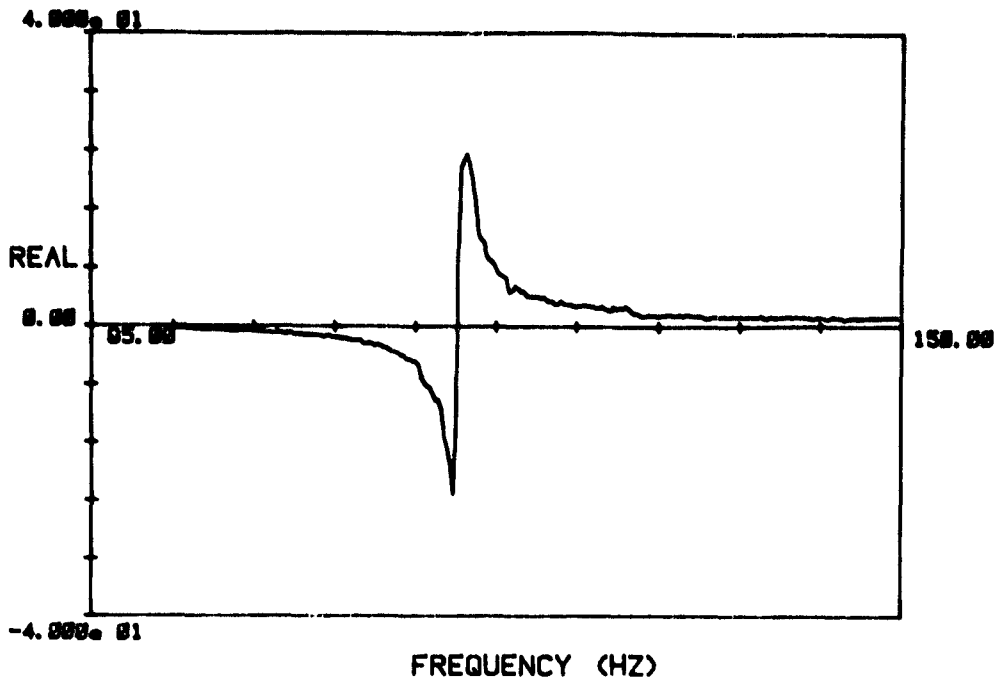

Figure 11d. Real Part of H_{11}. Configuration (3).

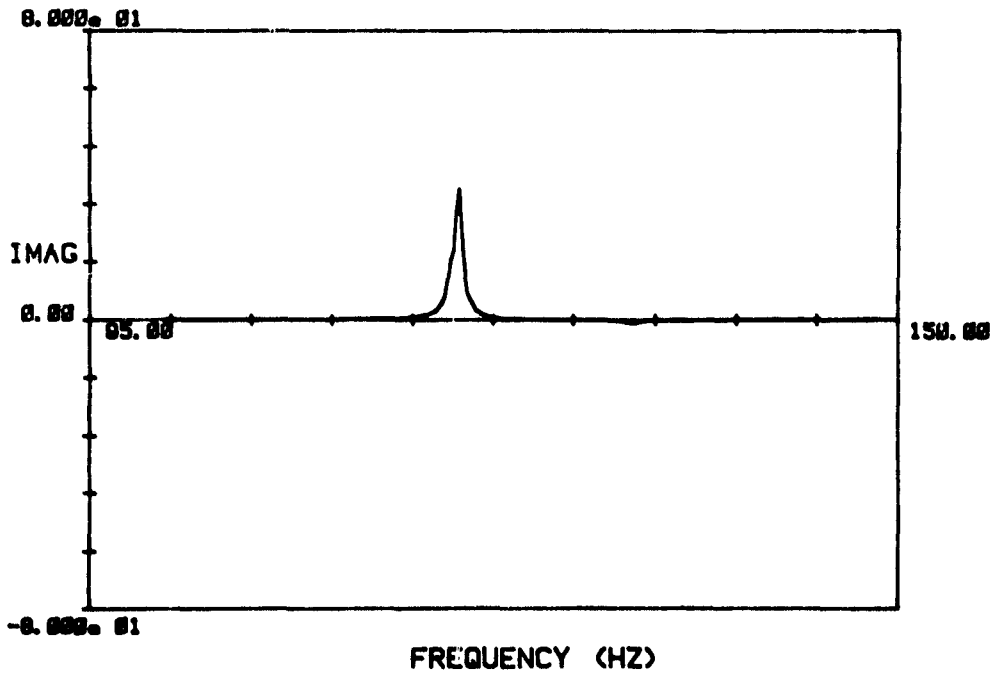

Figure 11e. Imaginary Part of H_{11}. Configuration (3).

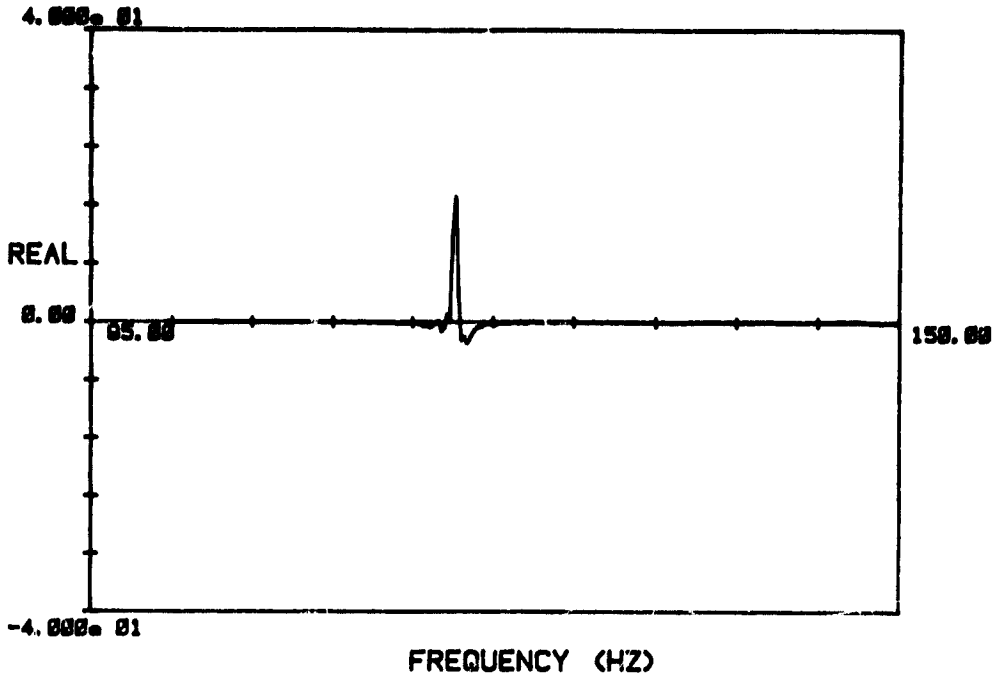

Figure 11f. Real Part of H_{61}. Configuration (3).

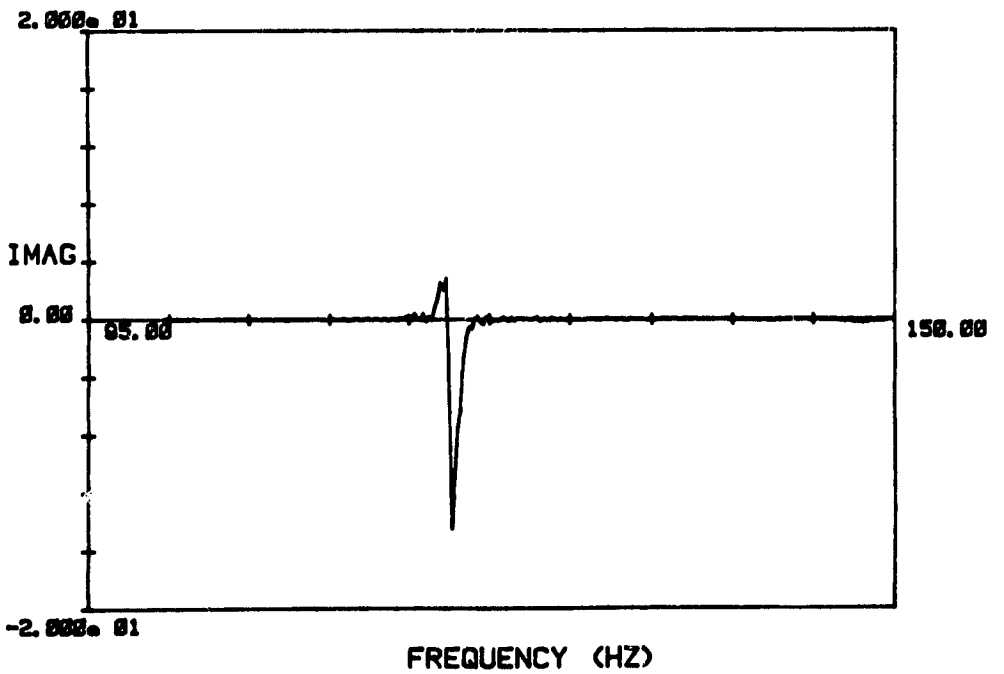

Figure 11g. Imaginary Part of H_{61}. Configuration (3).

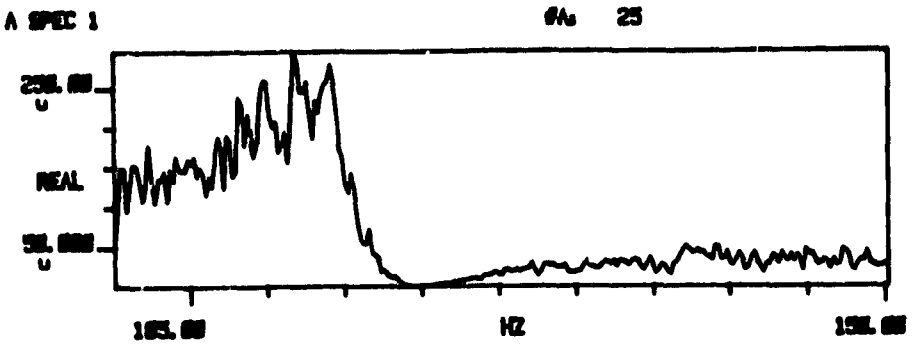

Figure 12a. Force Autospectrum. Single-shaker Test. Configuration (3).

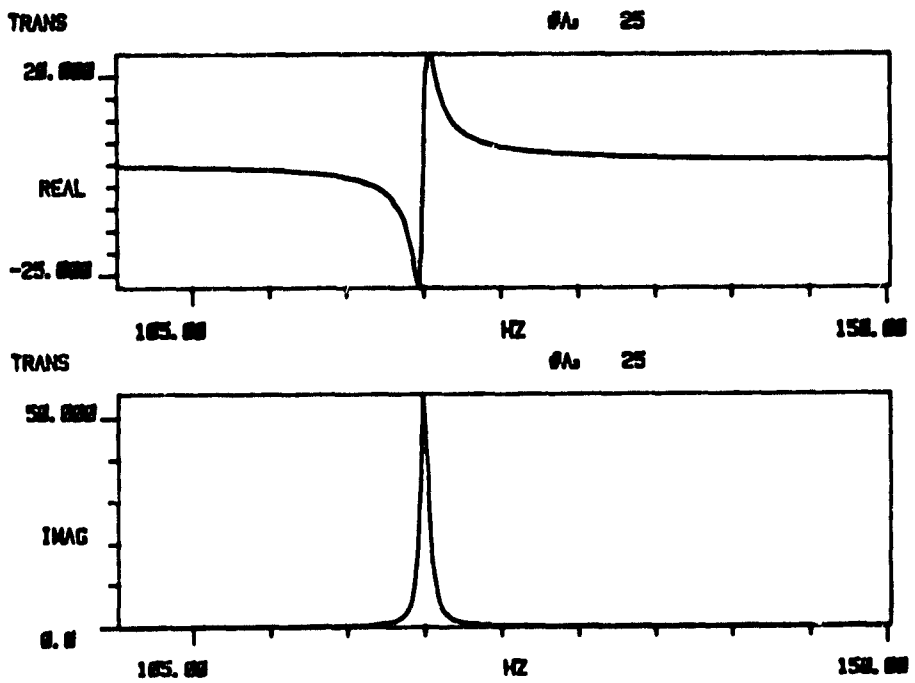

Figures 12b,c. H_{11}. Single-shaker Test. Configuration (3).

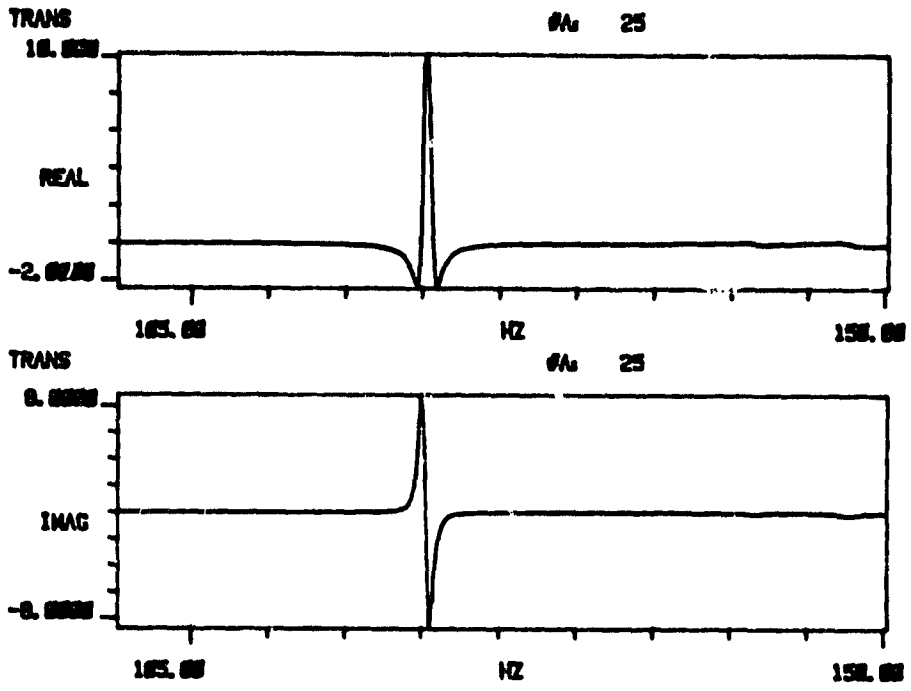

Figures 12d,e. H_{61}. Single-shaker Test.
Configuration (3).

Curve-Fitting:

The MDOF curve-fit algorithm of the MODAL-PLUS program of Structural Dynamics Research Corporation has been used to curve-fit experimental FRF's. Figures 13(a) and 13(b) show the MDOF curve-fits of the dual-shaker FRF's of Figures 11(d) through 11(g). Table 2 lists the roots determined by the curve-fit algorithm.

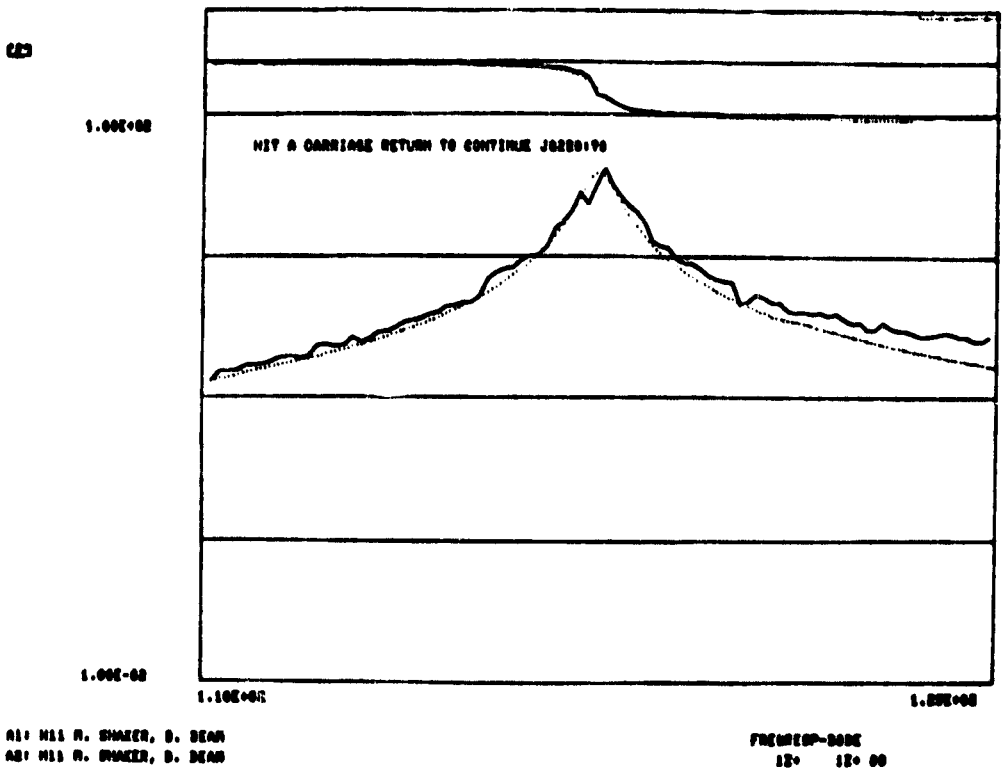

Figure 13a. MDOF Curve-fit of H_{11}. Configuration (2).

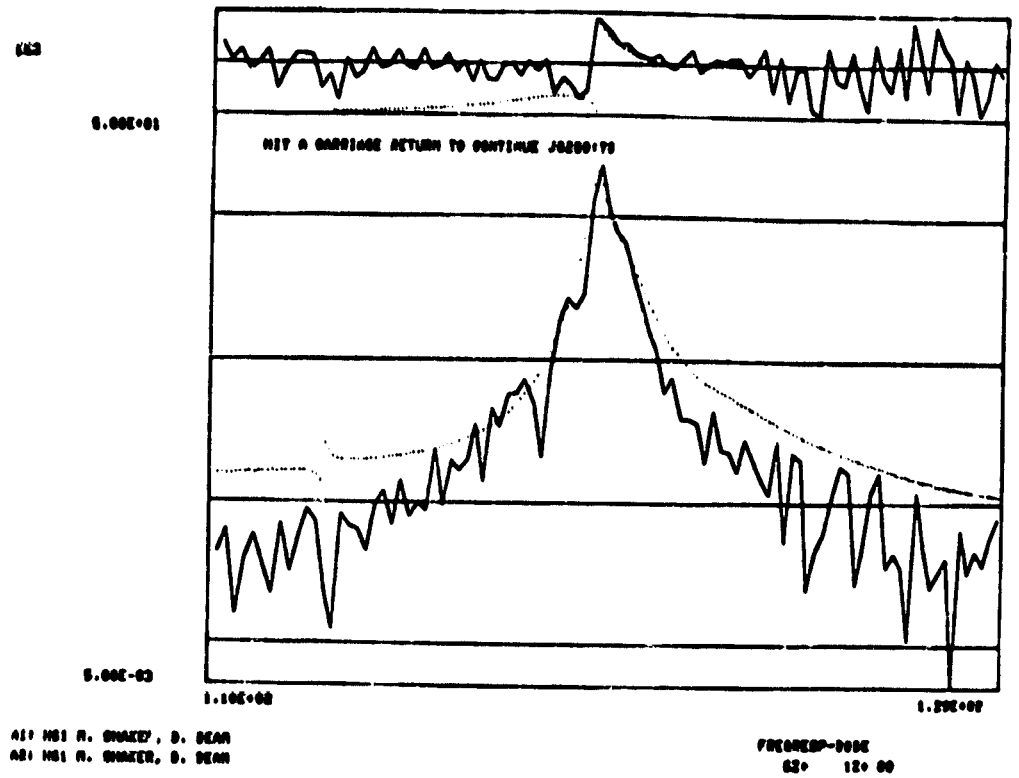

Figure 13b. MDOF Curve-fit of H_{61}. Configuration (2).

Estimated Roots	(1Z+ 1Z+)		
Root	Frequency	Damping	Amplitude	Phase
1	110.0	0.1349E-01	1.819	-0.9352E-06
2	117.2	0.1128E-01	0.2153E-01	1.563
3	119.0	0.3489E-02	104.2	1.490
4	119.7	0.6401E-01	36.21	-1.223
5	123.5	0.4142E-02	0.5937	1.963
6	129.1	0.1641E-02	0.1337	-3.142

Estimated Roots	(6Z+ 1Z+)		
Root	Frequency	Damping	Amplitude	Phase
1	110.2	0.7227E-01	2.689	0.7931E-07
2	112.5	0.3728E-03	0.3629E-01	1.474
3	118.8	0.1139E-02	18.20	-0.3084E-01
4	119.5	0.5012E-02	17.73	-2.867
5	121.7	0.9861E-02	1.115	-2.053
6	129.1	0.1089E-01	0.2363	-3.142

Table 2. Estimated Roots for H_{11} and H_{61}.

Modal Tuning:

As noted earlier, both the standard Asher Method of modal tuning, which is based on Equations (18) and (19), and a minimum coincident response method based on Equations (23) and (25) have been employed. They have been applied to the following data: (1) analytical 2DOF FRF's, (2) single-shaker FRF's (no curve-fitting), and (3) dual-shaker FRF's (no curve-fitting). Work is currently in progress on using curve-fit FRF's for modal tuning.

Figure 14 shows the simple 2DOF analytical model used to test the frequency separation capabilities of the standard Asher Method and the minimum coincident response method. Table 3 illustrates the fact that the minimum coincident response method was able to separate the modes for the (5.00, 5.05) Hz case but not for the (5.00, 5.01) Hz case. The standard Asher Method, on the other hand, was able to separate the modes for the (5.00, 5.01)Hz case. Table 4 shows the frequencies obtained by applying standard Asher tuning and minimum coincident response tuning to single-shaker and dual-shaker FRF's obtained for the experimental model shown in Figure 9. It has not yet been possible to complete the modal tuning calculations based on curve-fits of the single-shaker and dual-shaker experimental data.

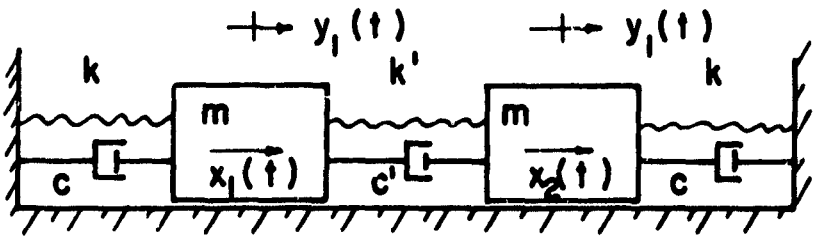

Figure 14. 2DOF Analytical Model

Method \ Mode	Mode 1 5.00Hz	Mode 2 5.01Hz	Mode 1 5.00Hz	Mode 2 5.05Hz
Standard Asher Method	5.0039	5.0156	*	*
Minimum Coincident Response Method	5.0039	-	5.0039	5.0508
*Not computed				

Table 3. Modal Tuning Based on 2DOF Analytical FRF's

Method	Test Type	Mode 1	Mode 2
Standard Asher Method	Single-Shaker	119.727	119.922
	Dual-Shaker	119.727	120.117
Minimum Coincident Response Method	Single-Shaker	119.922	-
	Dual-Shaker	119.727	120.117

Table 4. Modal Tuning Based on Experimental FRF's

Summary and Conclusions

A modal testing program consisting of data acquisition and FFT processing, curve-fitting, modal tuning, mathematical modeling, and computer-controlled testing has been outlined. Both single-shaker and dual-shaker methods of data-acquisition are permitted. An experimental model and several analytical models have been developed for use in verifying steps in the modal testing program. Frequency response functions of the experimental model have been acquired using both single-shaker and dual-shaker methods. The particular lightly-coupled structure which was tested led to considerable difficulty in obtaining good FRF's using two shakers. Further work is needed in order to develop multishaker test procedures to the state of usefulness currently enjoyed by single-shaker testing.

Computer programs have been written to implement both standard Asher tuning and minimum coincident response tuning as means of refining modal parameter estimates through the use of actual or simulated multi-shaker FRF's. Based on the application of both tuning procedures to analytically-formulated FRF's and to experimentally-acquired FRF's, it appears that the standard Asher Method may be able to separate modes in situations where the minimum coincident response method "breaks down." Further research is needed to determine the limitations of both of these tuning procedures.

Two phases of the proposed modal test program have not yet been addressed. These are mathematical modeling and computer-controlled testing. These phases will be addressed in future research.

References

1. R. R. Gold and W. L. Hallauer, Jr., "Modal Testing with Asher's Method Using a Fourier Analyzer and Curve Fitting," Proc. 25th International Instrumentation Symposium, The Instrument Society of America, May 7-10, 1979, pp. 185-192.

2. R. R. Ensminger and M. J. Turner, "Structural Parameter Identification from Measured Vibration Data," AIAA/ASME/ASCE/AHS 20th Structures, Dynamics and Materials Conference, St. Louis, April, 1979, Paper No. 79-0829, pp. 410-416.

3. Asher, G. W., "A Method of Normal Mode Excitation Utilizing Admittance Measurements," Proc. National Specialists' Meeting on Dynamics and Aeroelasticity, Ft. Worth, published by Inst. of Aeronautical Science, 1958, pp. 69-76.

4. R. R. Craig, Jr. and Y-W. T. Su, "On Multiple Shaker Resonance Testing," AIAA Journal, Vol. 12, no. 7, 1974, pp. 924-931.

5. R. J. Allemang, Investigation of Some Multiple Input/Output Frequency Response Function Modal Analysis Techniques, Ph.D. Dissertation, Univ. of Cincinnati, 1980.

6. R. J. Allemang, et. al., Using Dual-Input Random Excitation Modal Analysis, Final Report for Eglin Structural Dynamics Laboratory, 1981.

7. J. S. Bendat and Allan G. Pierson, Engineering Applications of Correlation and Spectral Analysis, Chapter 8, John Wiley & Sons, 1980.

8. M. Richardson, "Modal Analysis Using Digital Test Systems," Seminar on Understanding Digital Control and Analysis in Vibration Test Systems, The Shock and Vibration Information Center, Washington, D. C., May 1975.

9. R. R. Craig, Jr., SIR Antenna Studies, NASA Johnson Space Center, August, 1979 (informal report).

10. D. L. Brown, et. al., "Parameter Estimation Techniques for Modal Analysis," SAE Transactions, v. 88, sect. 1, 1979, pp. 828-846.

11. P. Ibañez, "Force Appropriation by Extended Asher's Method," Paper 760873, SAE Aerospace Engineering and Manufacturing Meeting, 1976.